Stochastic temporal timing for intracellular events to cross dynamically fluctuating thresholds

Baohua Qiu[1,2], Jiajun Zhang[1,2*], Tianshou Zhou[1,2*]

1 Guangdong Province Key Laboratory of Computational Science, Sun Yat-Sen University, Guangzhou, People's Republic of China **2** School of Mathematics, Sun Yat-Sen University, Guangzhou, People's Republic of China

* zhjiajun@mail.sysu.edu.cn(JJ); mcszhtsh@mail.sysu.edu.cn(TS)

Abstract

Timing of events, which is essential for many cellular processes, depends on regulatory proteins reaching a critical threshold that in general is dynamically fluctuating due to molecular interactions. Increasing evidence shows considerable cell-to-cell variation in the timing of key intracellular events among isogenic cells, but how expression noise and threshold fluctuations impact both threshold crossing and timing precision remain elusive. Here we first formulate stochastic temporal timing of events as a problem of the first passage time (FPT) to a fluctuating threshold and then transform this problem into a higher-dimensional FPT problem with some fixed threshold. Using a stochastic model of gene regulation, we show that (1) in contrast to the case of fixed threshold, threshold fluctuations can both accelerate response (i.e., shorten the time of threshold crossing) and raise timing precision (i.e., reduce timing variability), (2) there is an optimal mean burst size such that the timing precision is best, and (3) fast threshold fluctuations can perform better in accelerating response and reducing variability than slow threshold fluctuations. These results not only interpret recent experimental observations but also have broad implications for diverse cellular processes and in drug therapy.

Author summary

Increasing evidence shows substantial cell-to-cell variation in the timing of key intracellular events among isogenic cells, which has potential consequences on cellular functions and phenotypes. In general, this variation originates from the stochasticity of two different kinds: gene expression noise that is inherent due to low copy numbers and threshold fluctuations that are generated due to molecular interactions. However, it is unclear how these stochastic origins impact precision in the event timing and the time that regulatory proteins reach threshold levels (called arrival time). In order to reveal this impact, we perform analytical and numerical calculations for the first passage time distributions in a representative stochastic model of gene regulation where an event is triggered when the protein level crosses a dynamically fluctuating threshold. Counterintuitively, we find that fluctuating thresholds not only shorten arrival time but also raise timing precision in contrast to fixed thresholds, and fast threshold fluctuations can both shorten arrival time and reduce timing variability than slow threshold fluctuations. These findings can well explain recent experimental observations such as fractional killing of a cell population, cell apoptosis induced by dynamics of p53 in response to chemotherapy, and dynamic persistence of bacteria.

Introduction

The timing of events is essential for many biological processes [1]. On the one hand, some important cellular processes depend on precision in the timing of key intracellular events, e.g., cell fate decision presumably requires a precise control of gene expression timing [2–15], and the controls of cell cycle and circadian clocks require timing precision that can be crucial for the correct physiology [16–24]. Most of these processes are based on gene expression, e.g., an activated gene may be required to reach in a precise time a threshold level of gene expression that triggers a specific downstream pathway. On the other hand, fractional killing, a phenomenon occurring in, e.g., bacteria and drug therapy, relies on the time that relevant proteins reach threshold levels (called arrival time for brevity), e.g., exposure of an isogenic bacterial population to a cidal antibiotic typically fails to eliminate a small fraction of refractory cells [25], and cells must reach a

threshold level of p53 to execute apoptosis and this threshold increases with time [26]. Similarly, fractional killing of a cancer cell population by chemotherapy depends on arrival time: the shorter the arrival time is, the more are the cells killed, indicating the therapeutic efficacy is better. In short, timing precision and arrival time are two important indices measuring the event timing. Characterization of control strategies that reduces variability in the event timing or/and shortens arrival time is critically needed to understand both reliable functioning of diverse intracellular pathways that relies on precision in the timing and drug efficacy that depends on the time that drug-dependent regulatory proteins reach threshold levels.

In general, internal signals and environmental cues can induce the expression of one or several regulators, which in turn can trigger an appropriate cellular response when their concentrations reach critical threshold levels [2–26]. However, a gene may reach a critical threshold of expression with substantial cell-to-cell variability even among isogenic cells exposed to the same constant stimulus. This variability is a necessary consequence of the inherently stochastic nature of gene expression [27–32]. Apart from this internal stochastic origin of timing, dynamically fluctuating thresholds can also result in variability in the time required to reach a critical threshold level [9,12,26]. Such a kind of threshold has a strong biological background and is ubiquitous in biological regulatory systems. For example, consider a representative activity function of Hill type [33–36]

$$\text{Activation} = \frac{Z^n}{Z^n + K^n} \tag{1}$$

where n is a Hill coefficient, and $K = k_-/k_+$ represents a threshold (in fact a dissociation constant) of variable Z. In general, reaction rate k_+ or k_- is regulated by external signals that are stochastically generated due to biochemical reactions, e.g., $k_- = \alpha_1 S + \alpha_0$ where S, an external signal, is stochastically generated, α_0 and α_1 are positive constants. In this case, K is a dynamically fluctuating threshold of Z. For a gene whose expression has to reach a dynamically fluctuating threshold level, expression noise and threshold fluctuations can all lead to variability in the event timing. This raises questions: how these two stochastic origins impact threshold crossing, and which regulatory strategies can control variability in the event timing. Most previous studies have focused on the

first-passage properties of stationary threshold crossing [34–40], while comparatively very few studies have investigated how a dynamically fluctuating threshold impacts timing precision and arrival time theoretically [41–44] or experimentally [9, 12, 26].

In this article, we formulate the timing of intracellular events as a first passage time (FPT) problem, where an event is triggered when a stochastic process (in fact single-cell protein level) crosses a dynamically fluctuating threshold for the first time. Furthermore, we develop an analytical approach to estimate and simulate stochastic temporal timing of events in a model of gene regulation, and investigate how key system parameters (such as mean burst size, transcription and degradation rates) control timing precision and arrival time. In order to reveal the qualitative effects of these regulatory strategies, we compare results in the case of fixed thresholds with those in the case of dynamically fluctuating thresholds, finding that in contrast to the former, the latter not only accelerates threshold crossing but also keeps timing precision. This counterintuitive finding interprets recent experimental observations (e.g., many chemotherapeutic drugs kill only a fraction of cancer cells [25]; cell-to-cell variation in p53 dynamics leads to fractional killing [26]) and has broad implications for diverse cellular processes and in drug resistance.

Methods

Stochastic model formulation for FPT problems

First, we formulate the stochastic temporal timing of events as a problem of FPT to a dynamically fluctuating threshold. Let $\{X : X = X(t), t \geq 0 \mid X(0) = x\}$ be a temporally homogeneous stochastic process, and let $\{Y : Y = Y(t), t \geq 0 \mid Y(0) = y\}$ represent a dynamically fluctuating threshold (boundary or barrier). Without loss of generality, we set $x < y$. This setting is natural since Y represents the critical threshold that X will cross. Note that the union of two trajectories $X(t)$ and $Y(t)$, $\{(X, Y) : X = X(t), Y = Y(t), t \geq 0 \mid X(0) = x, Y(0) = y\}$ constitutes a new system. Define T as the time that trajectory X hits trajectory Y for the first time, that is,

$$T = \min\{t : X(t) = Y(t) | X(0) = x < Y(0) = y\} \tag{2}$$

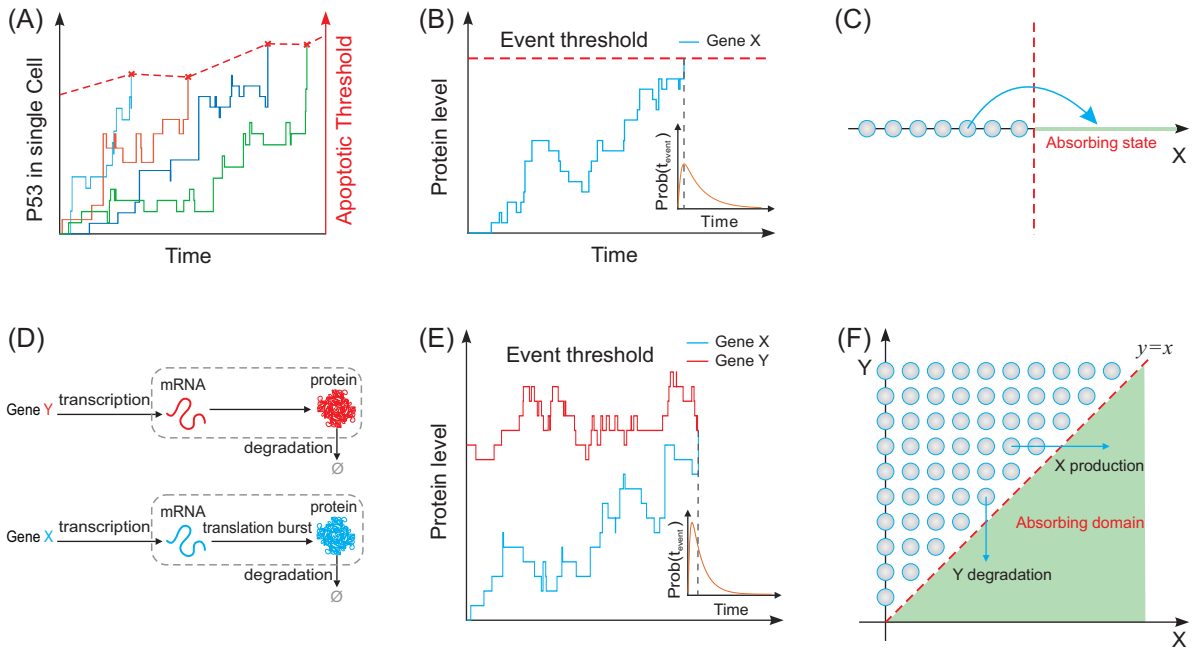

Fig 1. Threshold crossing can be modeled as a FPT problem. (A) A realistic example involving FPT, where cells must reach a threshold level of p53 to execute apoptosis and this threshold increases with time [26]. (B) The expression level of gene X changes over time, where the dashed red line represents a critical threshold that the gene product crosses, and the inset shows the FPT distribution. (C) Schematic for an absorbing domain of FPT, where the empty circles with arrow represents threshold crossing. (D) Two gene models, where the model for gene X assumes that the gene is expressed in a burst manner whereas that for gene Y assumes that the gene is expressed in a constitutive manner. (E) A FPT problem with a dynamically fluctuating threshold, where $Y(t)$ represents the threshold curve that $X(t)$ hits for the first time, and the inset shows the FPT distribution. (F) A one-dimensional FPT problem with a dynamically fluctuating threshold is transformed into a two-dimensional FPT problem with a fixed threshold. The shadow region represents an absorbing domain of FPT in the (X, Y) plane, defined by $D = \{(X, Y)|X \geq Y\}$, where an event is triggered once X crosses Y, the line of $y = x$ represents the boundary of region D, and arrows represent the possible directions of threshold crossing.

which is called FPT [45–48]. Apparently, T is a random variable since both $X(t)$ and $Y(t)$ are stochastic and depend respectively on initial x and y, referring to Fig 1(A).

Then, we transform an one-dimensional problem of FPT to a dynamically fluctuating threshold into a two-dimensional problem of FPT to a fixed threshold. For this, we introduce an absorption domain D, which consists of those points (X, Y) satisfying $X \geq Y$ in the (X, Y) plane, that is, $D = \{(X, Y)|X \geq Y\}$. In addition, we introduce a survival probability, $\mathbb{S}$, that the trajectory $\{(X(t), Y(t))\}$ starting from (x, y) at time $t = 0$ has not yet been absorbed into domain D at time t. Let $P_{X',Y'}(t)$ represent the probability that a two-dimensional system is at state (X', Y') at time t, that is,

$$P_{X',Y'}(t) = \text{Prob}\{X(t) = X', Y(t) = Y'|X(0) = x < Y(0) = y\}. \tag{3}$$

For convenience, $P_{X',Y'}(t)$ is sometimes denoted by $P_{S'}(t)$, i.e., $P_{S'}(t) = P_{X',Y'}(t)$, where $S' = (X', Y')$ represents state. Note that the survival probability is equal to the sum of the probabilities of all the states that does not belong to the absorbing region, i.e., $\mathbb{S} = \sum_{S \notin D} P_S(t)$. Denote by $f_T(t)$ the probability density function of the FPT, that is, $f_T(t) = \text{Prob}\{T \leq t\}$. In this paper, we are mainly interested in statistical properties of random variable T.

Statistical quantities of FPT distribution

Here, we first establish the relation between $f_T(t)$ and $\mathbb{S}$, and then give the formal expression of $f_T(t)$. Assume that all states $\{S(t) : t \geq 0\}$ with $S(t) = (X(t), Y(t))$ constitute a Markov process. Then, we have a forward master equation (FME) of the form [47, 48]

$$\frac{\partial \mathbf{P}(t)}{\partial t} = \mathbf{M}\mathbf{P}(t) \tag{4}$$

where $\mathbf{P}(t)$ is a column vector consisting of all $P_S(t)$, and $\mathbf{M}$ is a certain linear operator, depending a process of interest. Note that every component of $\mathbf{P}(t)$ is the probability that the system $\{S(t) : t \geq 0\}$ arrives at the absorbing domain D at time t, and that $\mathbf{M}$ is actually a state transition matrix. Let $P(S_f, t|S, t_0)$ be the probability that $S(t)$ reaches the absorbing state S_f at time t, given the initial state $S = S(t_0)$ at time t_0 with $S(t_0) = (x, y)$ ($t_0 = 0$ can be set). And let $\mathbb{S}(t, S_f|S, t_0)$ the survival probability that the state $S(t)$ starting from S at time t_0 has not yet been absorbed to state S_f at time t, i.e.,

$$\mathbb{S}(t, S_f|S, t_0) = \sum_{S' \neq S_f} P(S', t|S, t_0) \tag{5}$$

By definition, we have the relation $\text{Prob}\{T \leq t\} = 1 - \mathbb{S}(t, S_f|S, t_0)$. Thus, the probability density function of the FPT is given by (See the S1 Supporting Information for more details.)

$$f_T(t) = \mathbf{W}^{\mathrm{T}}\mathbf{P}(t) = \mathbf{W}^{\mathrm{T}} \exp(\mathbf{M}t)\mathbf{P}(0) \tag{6}$$

where $\mathbf{W}$ is the column vector of the transition rates from all accessible states to the absorbing state and the superscript T represents transpose [34, 36, 45–48].

Once the probability density function of the FPT, $f_T(t)$, is given or found, we can show that raw moments of random variable T are given by (see S1 Supporting

Information for derivation)

$$\langle T^k \rangle = \int_0^\infty t^k f_T(t)dt = k!(-1)^k \mathbf{e}^{\mathrm{T}}(\mathbf{M}^{-1})^k \mathbf{P}(0), k = 1, 2, \cdots, \tag{7}$$

where $\mathbf{e}^{\mathrm{T}} = [1, 1, \cdots, 1]$ is a constant vector. This indicates that the moments of FPT can be calculated directly based on the FME once the initial transition probabilities $\mathbf{P}(0)$ are set. In particular, the mean first-passage time (MFPT) is calculated according to

$$\mathrm{MFPT} = \langle T \rangle = -\mathbf{e}^{\mathrm{T}}\mathbf{M}^{-1}\mathbf{P}(0) \tag{8}$$

and the intensity of the noise in T (defined as the ratio of variance over the square of mean), which represents variability in the timing or reflects precision in the timing, is calculated according to

$$\mathrm{CV}_T = \frac{\langle T^2 \rangle - \langle T \rangle^2}{\langle T \rangle^2} = \frac{2\mathbf{e}^{\mathrm{T}}(\mathbf{M}^{-1})^2\mathbf{P}(0)}{[\mathbf{e}^{\mathrm{T}}\mathbf{M}^{-1}\mathbf{P}(0)]^2} - 1 \tag{9}$$

To calculate MFPT and CV_T, the key is to calculate the inverse of matrix $\mathbf{M}$. In the following, "Timing Mean" and "Timing varibility" are measured by MFPT and CV_T, respectively. And other higher order moments such as skewness and kurtosis can also be formally given, detailed in the S1 Supporting Information.

For clarity and in order to reveal how dynamically fluctuating thresholds impact both timing precision and threshold crossing, we consider a simple yet representative model of stochastic gene expression (referring to Fig 1(D)), where a timing event is triggered once the expression level of a gene (its product is denoted by X) crosses the expression level of another gene (its product is denoted by Y) for the first time. Assume that the X molecules are produced in a burst manner whereas the Y molecules are generated in a constitutive manner. We use the produced counts of protein molecule X to construct a stochastically fluctuating threshold to the molecule number of protein X. Let $Y(t) \in \{0, 1, 2, \cdots\}$ denote the level of protein Y at time t, and assume that $Y(t)$ follows a Poisson distribution with two characteristic parameters $g_{\mathrm{y}}^{(n)}$ (where superscript (n) means that feedback regulation is considered and may be omitted in the absence of feedback regulation) and d_{y} which represent respectively the transcription and degradation rates of protein Y when $Y(t) = n$. Let $X(t) \in \{0, 1, 2, \cdots\}$ denote the level

of protein X at time t, and assume that protein X is generated with a Poisson rate $g_{\mathrm{x}}^{(m)}$ (where the meaning of superscript (m) is similar to that of superscript (n)), and degrades at a constant rate d_{x}. The translation burst approximation is based on the assumption of short-lived mRNAs, that is, each mRNA degrades instantaneously after producing a burst of B protein molecules, where B follows a geometric distribution [49–52], that is

$$P_B(B=k) = \frac{b^k}{(1+b)^{k+1}}, k = 0, 1, 2, \cdots . \tag{10}$$

with b representing the average burst size. Then, we can show $P_B(B \geq k) = (b/(1+b))^k$, $k = 0, 1, 2, \cdots$. In what follows, we denote $P_{B=k} \equiv P_B(B=k)$ and $P_{B\geq k} \equiv P_B(B \geq k)$ for simplicity.

The time evolution of $(X(t), Y(t))$ starting from $(X(0) = m, Y(0) = n)$ with $m < n$ at time t can be described through the following probabilities of timing events in the next infinitesimal time $[t, t+dt)$

$$\begin{aligned}
&P(X(t+dt) = m+B, Y(t+dt) = n | X(t) = m, Y(t) = n) = g_{\mathrm{x}}^{(m)} dt;\\
&P(X(t+dt) = m-1, Y(t+dt) = n | X(t) = m, Y(t) = n) = m d_{\mathrm{x}} dt;\\
&P(X(t+dt) = m, Y(t+dt) = n+1 | X(t) = m, Y(t) = n) = g_{\mathrm{y}}^{(m)} dt;\\
&P(X(t+dt) = m, Y(t+dt) = n-1 | X(t) = m, Y(t) = n) = n d_{\mathrm{y}} dt.
\end{aligned} \tag{11}$$

An event occurs if the cumulative number of proteins molecule X reaches the number of protein molecule Y. The relation between the protein molecules X and Y can be considered as a trajectory in the domain $\{(X,Y)|X = X(t) < Y(t) = Y\}$. The corresponding FME describing the time evolution of protein pair X and Y can be described as the following master equation [34, 36, 45–48]

$$\begin{aligned}
\frac{dP_{m,n}(t)}{dt} = &\sum_{i=0}^{m-1} g_{\mathrm{x}}^{(i)} P_{B=m-i} P_{i,n}(t) + g_{\mathrm{y}} P_{m,n-1}(t) + (m+1) d_{\mathrm{x}} P_{m+1,n}(t)\\
&+ (n+1) d_{\mathrm{y}} P_{m,n+1}(t) - \left(g_{\mathrm{x}}^{(m)} P_{B\geq 1} + g_{\mathrm{y}} + m d_{\mathrm{x}} + n d_{\mathrm{y}}\right) P_{m,n}(t)
\end{aligned} \tag{12}$$

where $m < n$. Note that this equation is actually another form of Eq(4). Then, the FPT

distribution can be formally expressed as

$$f_T(t) = \sum_{m\geq 0}(m+1)d_{\mathrm{y}}P_{m,m+1}(t) + \sum_{n>m\geq 0} g_{\mathrm{x}}^{(m)} P_{B\geq n-m}P_{m,n}(t) \tag{13}$$

It is worth pointing out that the molecule number of protein X or Y may be infinite in theory, implying that $\mathbf{M}$ in Eq(4) is an infinite-dimensional matrix. Therefore, Eq(7), Eq(8) and (9) have only theoretical significance since they give only the formal expressions of FPT distribution and statistical quantities, respectively. Owing to such infinity, the FPT problem we study here is essentially different from a traditional FPT problem in which matrix $\mathbf{M}$ is finitely dimensional due to the fixed threshold. The infinite-dimensional FPT problem is in general intractable, and it is thus needed to develop computational methods. Here we propose a so-called truncation approach to solve this tough problem. This approach is developed based on the finite state projection [19], seeing the next subsection for details.

An efficient method for solving the problem of FPT to a fluctuating threshold

(A) Algorithm description

For clarity, we use the above gene model to introduce a truncation method although this method can be generic and applied to more complex cases.

First, the finite state projection approach [53] tells us that if matrix $\mathbf{M}$ is replaced by a $k\times k$ sub-matrix $\mathbf{M}$ with large k, then the approximation $\mathbf{P}(t)\approx \exp(\mathbf{M}_k t)\tilde{\mathbf{P}}(0)$ holds, where $\tilde{\mathbf{P}}(0)$ replaces the original $\mathbf{P}(0)$ in some order. As a result, the state vector (X_i, Y_i) constitutes a finite state projection, where $i\in 1,2,\cdots,k$.

Second, we define $\Gamma_k = \mathbf{e}^{\mathrm{T}}\exp(\mathbf{M}_k t)\tilde{\mathbf{P}}(0)$ which represents the sum of the components of vector $\mathbf{P}(t)$. According to the finite state projection approach [19], we can prove that if $\Gamma_k \geq 1-\varepsilon$ with ε being a small positive number, then

$$\exp(\mathbf{M}_k t)\tilde{\mathbf{P}}(0) \leq \mathbf{P}(t) \leq \exp(\mathbf{M}_k t)\tilde{\mathbf{P}}(0) + \varepsilon\mathbf{e} \tag{14}$$

Based on the above analysis, we develop the following truncation algorithm:

Inputs Propensity functions and stoichiometry for all reactions.

Initial probability density vector $\tilde{\mathbf{P}}(0)$

Final time of interest, t_f.

Total amount of acceptable error, ε

Initial finite set of states, (X_0, Y_0).

Initialize a counter, $k = 0$.

Step 0 Calculate $\mathbf{M}_k = \text{Submatrix}(\mathbf{M})$, which depends on (X_k, Y_k), and $\Gamma_k = \mathbf{e}^{\mathrm{T}} \exp(\mathbf{M}_k t)\tilde{\mathbf{P}}(0)$.

Step 1 If $\Gamma_k \geq 1 - \varepsilon$, **Stop**.

$\exp(\mathbf{M}_k t)\tilde{\mathbf{P}}(0)$ approximates the probability $\mathbf{P}(X_k, Y_k, t_f)$ with error ε.

Step 2 Add more states, $(X_{k+1}, Y_{k+1}) = \text{Expand}((X_k, Y_k))$, and take $k \leftarrow k + 1$.

Increment k and return to **Step 1**.

(B) The expression of matrix M

Owing to the effectiveness of the truncation approach proposed above, we may assume that matrix $\mathbf{M}$ is finitely dimensional (otherwise, we use finitely dimensional matrix, $\mathbf{M}_k$). To derive the expression of matrix $\mathbf{M}$ in the above gene model, we consider a special absorbing domain

$$D_1 = \{(X, Y)|X = X(t) \geq Y(t) = Y\} \tag{15}$$

The S1 Supporting Information performs analysis for other three kinds of absorbing domains.

We introduce two numerical cutoffs for the numbers of proteins X and Y: $X_{\max}$ for $X(t)$ and $Y_{\max}$ for $Y(t)$, and without loss of generality, assume that $X_{\max} = Y_{\max} = C$ (a known integer). Therefore, $m \in \{0, 1, 2, \cdots, C - 1\}$ and $n \in \{1, 2, \cdots, C\}$ for the above gene model (see Fig 1(F)). That means that the corresponding finite state space for stochastic process can be considered as follows

$$\Omega = \{(m, n)|m < n, m = 0, 1, 2, \cdots, C - 1, n = 1, 2, \cdots, C\} \tag{16}$$

For convenience, we rewrite vector $\mathbf{P}(t)$ as $\mathbf{P} = [\mathbf{P}_{*,1}, \mathbf{P}_{*,2}, \mathbf{P}_{*,3}, \cdots, \mathbf{P}_{*,C}]^{\mathrm{T}}$, with $\mathbf{P}_{*,k}$ represents $\mathbf{P}_{*,k} = [P_{0,k}, P_{1,k}, \cdots, P_{k-1,k}, 0, \cdots, 0]$, $k \in \{1, 2, \cdots, C\}$, omitted here time t. Also for convenience, we introduce an operator, denoted by $\mathbb{L}^{(i)} (i = 1, 2, \cdots, n)$, which acts on matrix with the operation rule being below: $\mathbb{L}^{(i)}\mathbf{M} = \mathbf{M}^{(i)}$, where $\mathbf{M}^{(i)}$ is a matrix whose order is the same as $\mathbf{M}$ but some components are zero, e.g., if $\mathbf{M} = (a_{ij})_{3\times 3}$, we obtain $\mathbb{L}^{(2)}\mathbf{M} = \mathbf{M}^{(2)} = (b_{ij})_{3\times 3}$ where $(b_{ij})_{2\times 2} = (a_{ij})_{2\times 2}$ and the other elements are equal to zero. Thus, matrix $\mathbf{M}$ in the above gene model can be expressed as the following form

$$\mathbf{M} = \begin{pmatrix} \mathbf{D}_1 & \mathbf{U}_1 & & & & \\ \mathbf{L}_1 & \mathbf{D}_2 & \mathbf{U}_2 & & & \\ & \mathbf{L}_2 & \mathbf{D}_3 & \mathbf{U}_3 & & \\ & & \ddots & \ddots & \ddots & \\ & & & \mathbf{L}_{C-2} & \mathbf{D}_{C-1} & \mathbf{U}_{C-1} \\ & & & & \mathbf{L}_{C-1} & \mathbf{D}_C \end{pmatrix} \tag{17}$$

where

$$\begin{cases} \mathbf{U}_i = (i+1)\mathbb{L}^{(i)}(d_{\mathrm{y}}\mathbf{I}_C), & i = 1, 2, \cdots, C-1; \\ \mathbf{D}_i = \mathbb{L}^{(i)}[\mathbf{M}_{g_{\mathrm{x}}} + \mathbf{M}_{d_{\mathrm{x}}} - (g_{\mathrm{y}} + id_{\mathrm{y}})\mathbf{I}_C], & i = 1, 2, \cdots, C; \\ \mathbf{L}_i = \mathbb{L}^{(i)}(g_{\mathrm{y}}\mathbf{I}_C), & i = 1, 2, \cdots, C-1. \end{cases}$$

Here $\mathbf{I}_C$ is the $C \times C$ identity matrix. And the matrix $\mathbf{M}_{d_{\mathrm{x}}} = d_{\mathrm{x}}\mathrm{diag}([1, 2, \cdots, C-1], 1) - d_{\mathrm{x}}\mathrm{diag}([0, 1, \cdots, C-1], 0)$, where symbol $\mathrm{diag}(\mathbf{v}, k)$ represents that the elements of vector $\mathbf{v}$ are placed on the kth diagonal. Note that $k = 0$ represents the main diagonal, $k > 0$ is above the main diagonal, and $k < 0$ is below the main diagonal. Moreover, note that $\mathbf{M}_{g_{\mathrm{x}}} = g_{\mathrm{x}}\mathbf{M}_{\mathrm{burst}}$, where $\mathbf{M}_{\mathrm{burst}} = -P_{B\geq 1}\mathbf{I}_C + \sum_{k=1}^{C-1} P_{B=k}\mathrm{diag}(\mathbf{e}_{C-k}^{\mathrm{T}}, -k)$. In the case of feedback, implying that g_{x} depends on the molecule number (m) of protein X, then $\mathbf{M}_{g_{\mathrm{x}}^{(m)}} = \mathbf{M}_{\mathrm{burst}}\mathbf{G}$, where $\mathbf{G} = \mathrm{diag}([g_{\mathrm{x}}^{(0)}, g_{\mathrm{x}}^{(1)}, \cdots, g_{\mathrm{x}}^{(C-1)}], 0)$. (See the S1 Supporting Information for the formal expressions of these matries).

(C) The expression of FPT distribution $f_T(t)$

With the setting of a numerical cutoff (C), the FPT distribution in Eq (6) can be rewritten as (See the S1 Supporting Information for more details)

$$\begin{aligned} f_T(t) &= \sum_{m=0}^{C-1}(m+1)d_{\mathrm{y}}P_{m,m+1}(t) + \sum_{n=1}^{C}\sum_{m=0}^{n-1} g_{\mathrm{x}}^{(m)} P_{B\geq n-m} P_{m,n}(t) \\ &= \mathbf{W}_{d_{\mathrm{y}}}^{\mathrm{T}}\mathbf{P}_{m,n}(t) + \mathbf{W}_{g_{\mathrm{x}}}^{\mathrm{T}}\mathbf{P}_{m,n}(t) \\ &\equiv \mathbf{W}^{\mathrm{T}}\mathbf{P}_{m,n}(t) \end{aligned} \tag{18}$$

where $\mathbf{W} = [\mathbf{W}_1^{\mathrm{T}}, \cdots, \mathbf{W}_C^{\mathrm{T}}]^{\mathrm{T}}$ with $\mathbf{W}_n = nd_{\mathrm{y}}\mathbf{1}_n + \sum_{m=0}^{n-1} g_{\mathrm{x}}^{(m)} P_{B\geq n-m}\mathbf{1}_{m+1}, n = 1, 2, \cdots, C$. Here we define a column vector of length C $\mathbf{1}_i = (0, \cdots, 0, 1, 0, \cdots, 0)^{\mathrm{T}}$ in which the only ith element is equal to 1 and other elements is all zero.

Given a certain $\mathbf{P}(0)$, mean FPT and noise CV_T can be calculated by Eq(8) and Eq(9) respectively, where the the key is to calculate the inverse of matrix $\mathbf{M}$. In contrast, the FPT distribution $f_T(t)$ is easily calculated through Eq(18). In a word, through the calculation of these quantities, we can analyze characteristics of timing events with fluctuating thresholds, including the first passage time and variability in the timing. For a sake of simplicity, we will not consider feedback regulation implying that $g_{\mathrm{x}}^{(m)} = g_{\mathrm{x}}$, and $g_{\mathrm{y}}^{(n)} = g_{\mathrm{y}}$ are independent of m and n, respectively.

(D) The effectiveness of the truncation algorithm

In order to verify the effectiveness of the truncation algorithm proposed above, we perform numerical calculation using the gene model described in Fig 1D. Numerical results are shown in Fig 2.

Fig 2(A) and 2(B) demonstrate the dependence of the mean FPT and the timing variability on the cutoff of the protein X number, respectively. We observe with increasing the cutoff constant, both can well approximate the "exact" values (empty circles) obtained by the Gillespie stochastic algorithm [20] with increasing the cutoff constant. For example, the approximate mean FPT is nearly equal to the exact mean FPT at $X_{\max} \approx 23$ whereas the approximate timing variability is nearly equal to the timing variability at $X_{\max} \approx 25$. Fig 2(C) demonstrates the distribution of FPT for a particular cutoff constant $X_{\max} \approx 30$.

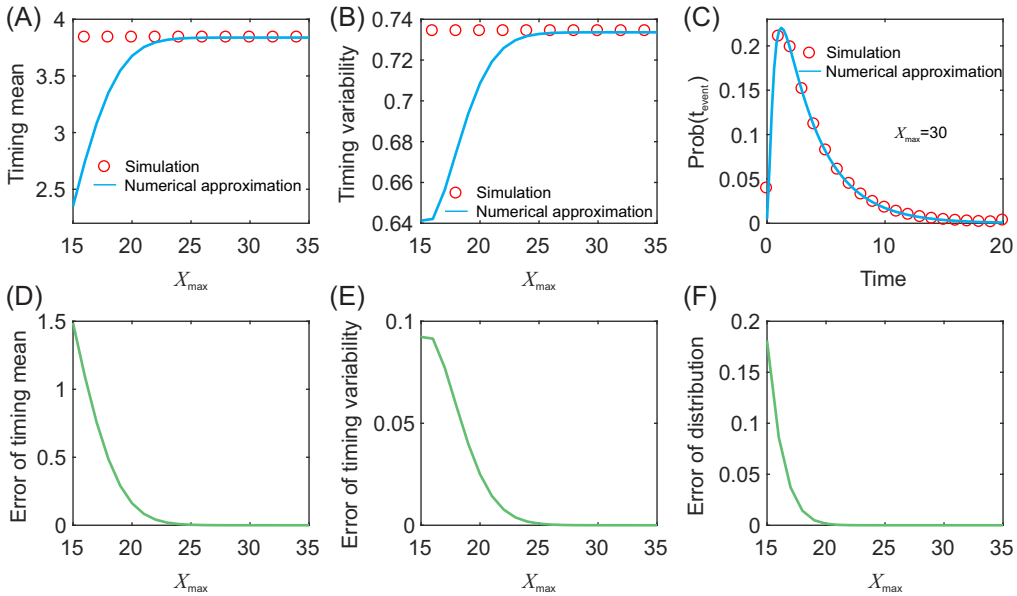

Fig 2. Verification of the effectiveness of the truncation algorithm with the model described in Fig 1(D). (A) Timing mean as of a function of $X_{\max}$, (B) Timing variability as a function of $X_{\max}$. (C) The FPT distribution for $X_{\max} = 30$. (D) The difference between simulation and approximate results of timing mean as a function of $X_{\max}$. (E) The difference between exact and approximate results of timing variability as a function of $X_{\max}$. (F) The Kullback–Leibler divergence between exact and approximate FPT distribution as a function of $X_{\max}$. In (A)-(F), empty circles represent the results obtained by the Gillespie stochastic simulation and are therefore viewed as "exact", whereas the curve represents the result obtained by our algorithm and are therefore viewed as "approximate". The parameter values are $g_{\mathrm{x}} = 5$, $d_{\mathrm{x}} = 1$, $b = 1$, $g_{\mathrm{y}} = 10$, $d_{\mathrm{y}} = 1$, the mean value of Y (i.e., the mean threshold) is set as $Y_{\mathrm{threshold}} = 10$, and the range of X is set as $X_{\max} = 15 \sim 35$.

Fig 2(D) demonstrates the dependence of the difference between the exact mean FPT obtained by the Gillespie stochastic algorithm [54] and the approximate mean FPT obtained by the finite state projection [53] on the cutoff constant $X_{\max}$. We observe that this difference quickly tends to zero as the cutoff constant is beyond some value. The similar change tendency holds for timing variability, referring to Fig 2(E). In addition, Fig 2(F) more clearly demonstrates that two kinds of FPT distributions obtained are in agreement since the Kullback–Leibler divergence between them tends to zero as the cutoff constant $X_{\max}$ increases, further verifying the effectiveness of the proposed truncation algorithm.

Results

Threshold fluctuations can both accelerate response and enhance precision

First, we introduce the conception of event threshold for convenience. By event threshold we mean that the average level of protein Y is equal to the ratio of the generation rate (g_{y}) over the degradation rate (d_{y}), e.g., the event threshold $Y_{threshold} = g_{\mathrm{y}}/d_{\mathrm{y}}$. Thus, an event threshold is nothing but a fixed threshold in the deterministic case (i.e., in the case of no fluctuations), which is equal to $g_{\mathrm{y}}/d_{\mathrm{y}}$. In the case of fluctuations, however, an event threshold may not be equal to the fixed threshold due to the effect of stochastic fluctuations.

Then, in order to show how fluctuating thresholds impact the timing of events, we plot Fig 3 where numerical results in the case of fixed threshold are also shown for comparison. From Fig 3(A), we observe that the curve for the dependence of mean FPT on event threshold in the case of fluctuations is always below the curve for the dependence of the mean FPT on event threshold in the case of no fluctuations, implying that threshold fluctuations always shorten the time that the regulatory proteins reach a critical threshold, or accelerate the response of intracellular events to external cues. As a supplement of Fig 3(A), Fig 3(B) demonstrates the dependence of the difference between the mean FPT in the case of fixed threshold and that in the case of fluctuating threshold, on event threshold. We observe that this difference is a monotonically increasing function of event threshold. The insets show two special FPT distributions, which correspond respectively to one empty circle and one triangle indicated in the figure.

Fig 3(C) demonstrates how event threshold impacts variability in the timing. From this figure, we observe that there is a critical event threshold (denoted by RP) such that the timing variability in the case of fluctuating threshold is smaller than that in the case of fixed threshold, as the event threshold is beyond RP but the former is larger than the latter as the event threshold is below RP. In other words, for a high event threshold, threshold fluctuations can reduce the timing variability or can raise the precision in the timing. In addition, we observe that there is an event threshold such that the variability in the timing is least in both cases of threshold (referring to

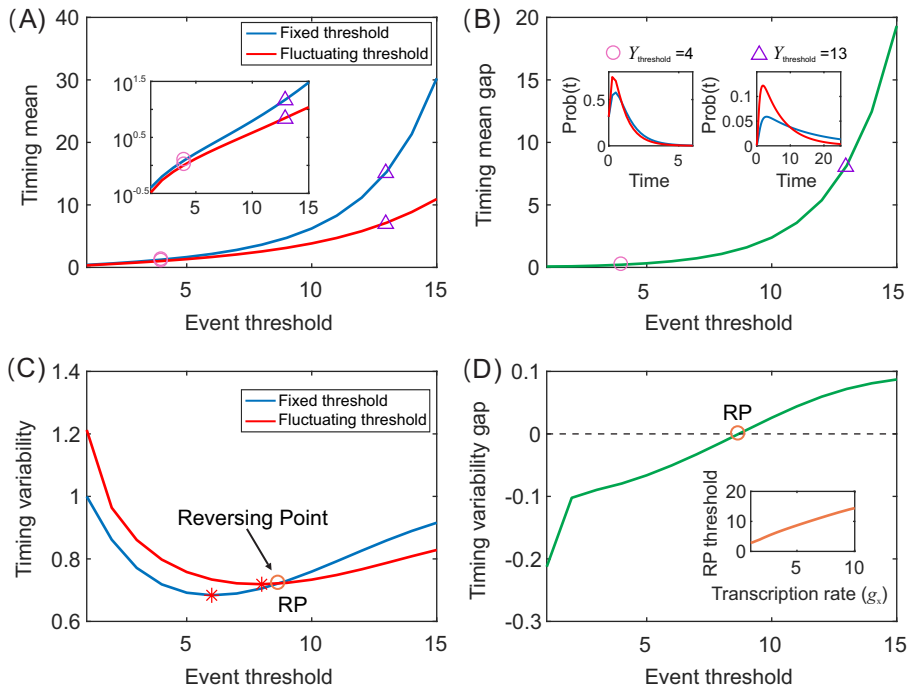

Fig 3. Comparison between the effects of fixed and fluctuating thresholds on timing. (A) Timing mean as a function of event threshold for two different kinds of thresholds, where the inset shows timing mean as a function of event threshold on the logarithmic scale. (B) A different demonstration of the results in (A), showing the difference of timing mean in the case of fixed threshold minus that in the case of fluctuating threshold, where insets show FPT distributions for two different event thresholds (indicated by empty circle and triangle) corresponding to $Y_{\text{threshold}} = 4$ and $Y_{\text{threshold}} = 13$. (C) Timing variability as a function of event threshold for two different kinds of thresholds, where the empty circle is the crossing point of two curves, and stars represent the critical threshold that makes timing variability reach the minimum. (D) As a supplement of (C), the difference of timing variability in the case of fixed threshold minus that in the case of fluctuating threshold, where the inset shows the critical threshold as a function of the transcription rate. In (A) and (C), the parameter values are $g_{\text{x}} = 5$, $d_{\text{x}} = 1$, $b = 1$, $X_{\max} = 30$, the fixed threshold is $Y_{\text{threshold}} = 10$, and the fluctuating threshold corresponds to $g_{\text{y}} = 10$ and $d_{\text{y}} = 1$. The inset in (D) corresponds to $d_{\text{x}} = 1$, $b = 1$, $g_{\text{y}} = 10$, $d_{\text{y}} = 1$, $g_{\text{x}} = 1 \sim 10$ and $X_{\max} = 30$.

the star indicated). This implies event threshold can make the timing precision reach optimality in both cases of fixed and fluctuating thresholds. Fig 3(D) is a different demonstration of the results in Fig 3(C), showing that the difference between the timing variability in the case of fixed threshold and that in the case of fluctuating threshold is a monotonically increasing function of event threshold. The inset shows the dependence of the critical event threshold on the transcription rate g_{x}, demonstrating that the critical event threshold increases with g_{x}.

In short, Fig 3(A) and 3(C) show one of our main results of this paper, that is,

dynamic fluctuations in threshold can accelerate the response of intracellular events to external cues by shortening the time that the regulatory proteins reach the critical threshold, fluctuations in high event thresholds can raise the precision in timing by reducing timing variability, and there is an even threshold such that the timing variability reaches optimality in both cases of fixed and fluctuating thresholds. These results imply that threshold fluctuations are an important factor affecting the timing of events.

Fast threshold fluctuations can accelerate response and enhance precision

In the above subsection, we have seen that fluctuations in thresholds have important influences on event timing. However, factors leading to such fluctuations may be diverse. Here we focus on investigating the effects of timescales on timing precision and mean FPT.

First, we give the definition of timescale. In our model, if the production rate (g_{x} or g_{y}) and the degradation rate (d_{x} or d_{y}) of protein X or Y are simultaneously enlarged by α_{x} or α_{y} times, then the factor α_{x} or α_{y} is defined as the timescale of protein X or Y. In general, the larger the factor α_{x} or α_{y} is, the larger are the fluctuations in protein X or Y. Therefore, α_{x} or α_{y} is an important factor leading to fluctuations in protein X or Y. Small α_{x} or α_{y} corresponds to the so-called slow fluctuations whereas large α_{x} or α_{y} to the so-called fast fluctuations. We can prove that the variability in event timing depends only on the ratio of α_y over α_x, independent of their sizes. See the S1 Supporting Information for details.

Then, we investigate the influence of timescales on mean FPT and variability in the even timing. Numerical results are shown in Fig 4. Specifically, Fig 4(A) and 4(D) demonstrate how timescales of proteins X and Y together affect the mean FPT and timing variability, respectively. We observe that the mean FPT in the case of small α_{x} (referring to the red dashed line) is always larger than that in the case of large α_{x}, independent of α_{y}. For a fixed yet small , the mean FPT in the case of small α_{y} (referring to the blue dashed line) is also larger than that in the case of large α_{y}. These imply that two kinds of timescales (internal for X and external for Y) can all significantly impact the mean FPT. Moreover, a larger external timescale leads to a less mean FPT

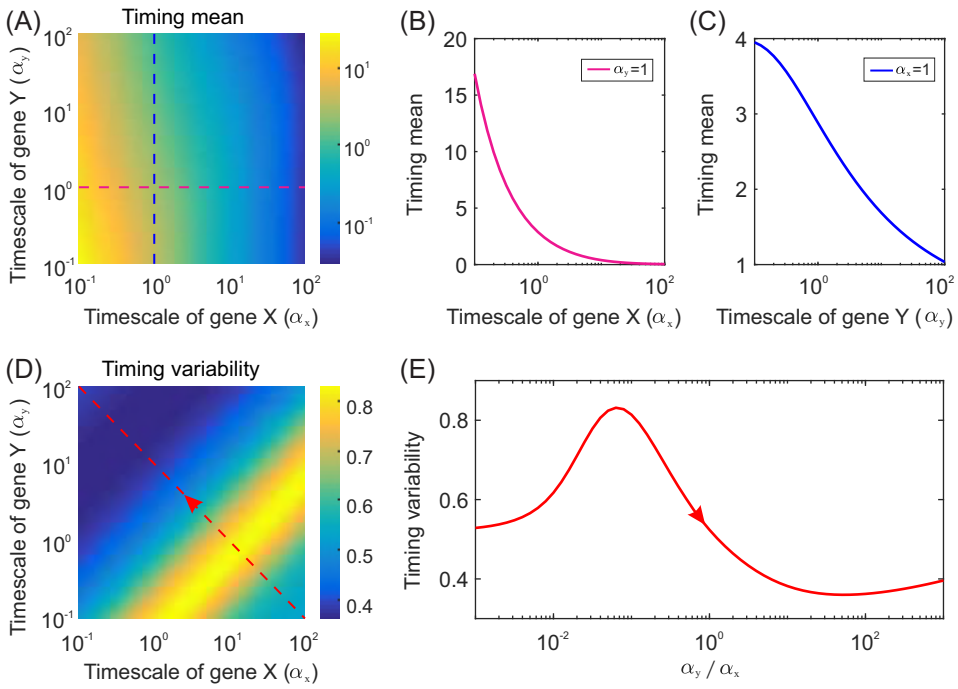

Fig 4. Effect of timescales on the timing of events, where α_x and α_y are respectively the common factors that the transcription and degradation rates of proteins X and Y are simultaneously enlarged. (A) Heatmap showing timing mean as a function of α_x and α_y. (B) Timing mean as a function of the timescale of protein X, where $\alpha_y = 1$. (C) Timing mean as a function of the timescale of protein Y, where $\alpha_x = 1$. (D) Heatmap showing timing variability as a function of the timescales of protein X and Y. (E) Timing variability as a function of the rate of the timescale of protein Y over that of protein X, where arrow is in agreement with that in (D). In (A)-(E), the parameter values are $g_x = 15$, $d_x = 1$, $b = 1$, $g_y = 20$, $d_y = 1$, $X_{max} = 50$.

for small internal timescale, but a smaller internal timescale leads to a larger mean FPT for small external timescale. On the other hand, this relationship is different in the case of timing variability, referring to Fig 4(D). We observe that there is a strip region (indicated by orange) in the plane of α_x and α_y, such that the variability in timing is largest. More precisely, if two boundary lines of this region are denoted as ℓ_1 and ℓ_2, which are described by $\alpha_y = a_1\alpha_x$ and $\alpha_y = a_2\alpha_x$, where a_1 and a_2 are all positive constants satisfying $a_1 < a_2$, then the timing variability below ℓ_1 or beyond ℓ_2 is less than that in the strip region, and the timing variability below ℓ_1 is less than that beyond ℓ_2 (referring to the dashed line with arrow). These indicate that in the outside of the strip region, if the timescale of protein Y is dominant, the timing variability becomes smaller, and conversely, if the timescale of protein X is dominant, the timing variability also becomes smaller. Since timescale factors α_x and α_y determine the noise in proteins

X and Y (called intrinsic and extrinsic noise) respectively, we can thus conclude that the intrinsic and extrinsic noise all can significantly contribute to the timing variability, but this contribution depends on which noise is dominant. This is an interesting phenomenon similar to the resonance that takes place as the external frequency is approximately equal to the external frequency [55].

From Fig 4(B) and 4(C), we observe that the mean FPT is a monotonically decreasing function of the timescale for proteins X and Y respectively, but the former is a convex-downward curve for a particular timescale of protein X, i.e., for $\alpha_{\mathrm{y}} = 1$, whereas the latter is fundamentally a line for a particular timescale of protein Y, i.e., for $\alpha_{\mathrm{x}} = 1$. Note that $\alpha_{\mathrm{x}} = 1$ and $\alpha_{\mathrm{y}} = 1$ correspond to blue and red dashed lines in Fig 4(A), respectively. The results shown in Fig 4(B) and 4(C) are practically special results shown in Fig 4(A). Fig 4(B) and 4(C) imply that internal and external (or threshold) timescales can all shorten the mean arrival time (i.e., the mean threshold crossing time). This further implies that timescales can speed up response.

Fig 4(E), which corresponds to the red dashed with arrow in Fig 4(D), shows how the rate between the timescales of proteins X and Y, $\gamma = \alpha_{\mathrm{y}}/\alpha_{\mathrm{x}}$, impacts the variability in the event timing. Interestingly, we observe that there is an optimal rate between external and internal timescales, $\gamma_{\mathrm{critical}}$, such as the timing variability is maximal, implying that the precision in the event timing is worst for this optimal timescale. Furthermore, the rate γ satisfying $\gamma < \gamma_{\mathrm{critical}}$ increases the timing variability whereas the rate γ satisfying $\gamma > \gamma_{\mathrm{critical}}$ fundamentally decreases the timing variability. The former implies that when the rate of the external timescale over the internal timescale, γ, is less than the critical value, $\gamma_{\mathrm{critical}}$, this rate weakens the precision in the event timing, and conversely, it fundamentally enhances this precision.

In a word, the timescales of proteins X and Y are two unneglectable factors in the timing of events since they can significantly affect the timing precision and MFPT. And there is a strip region in the plane of external and internal timescales such that the timing variability is largest (implying that the timing precision is worst).

Control strategies for the timing of events with fluctuating thresholds

The curves shown in Fig 4 correspond to a special value of the transcription or degradation rate of protein. However, these two rates can be regulated by external signals, leading to their changes in intervals. This raises a question: how these two rates impact the arriving time and the variability in the timing. Here we numerically analyze this impact, with results shown in Fig 5.

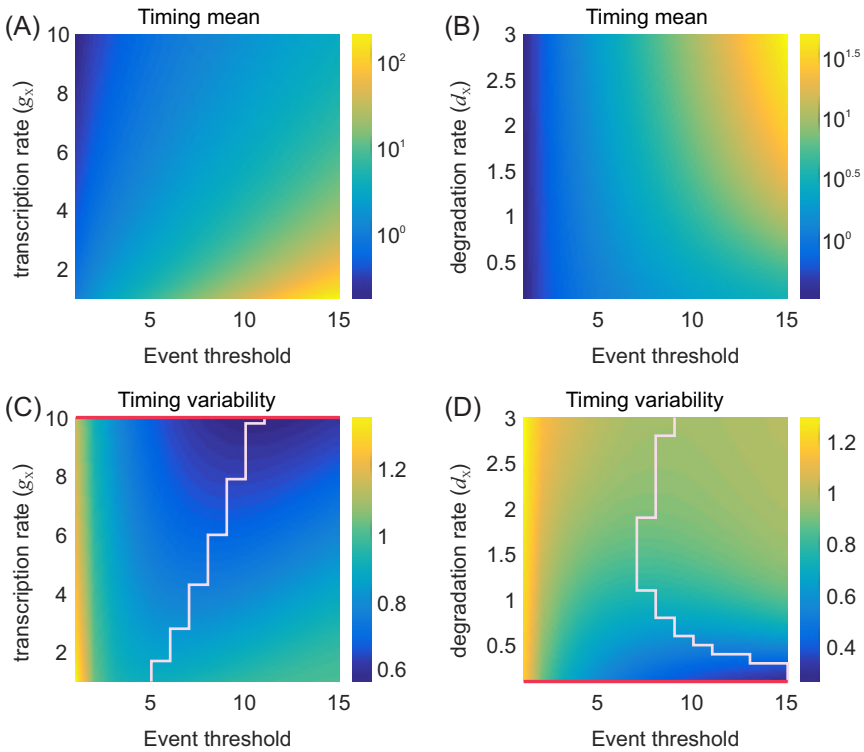

Fig 5. Influence of transcription or degradation rates on the timing of events. (A) Heatmap showing timing mean as a function of event threshold and transcription rate (g_x). (B) Heatmap showing timing mean as a function of event threshold and degradation rate (d_x). (C) Heatmap showing timing variability as a function of event threshold and transcription rate (g_x), where the stair-like line consists of the points corresponding to the star in Fig 3(D) where in a special value of g_x is used. (D) Heatmap showing timing variability as a function of event threshold and degradation rate (d_x), where the meaning of the stair-like line is similar to that in (C). Note that the event of threshold crossing has taken place when d_x is sufficiently small, which corresponds to the red line. In (A)-(D), the parameter values are set as $b = 1$, $g_y = 10$, $d_y = 1$, $X_{max} = 30$ and $Y_{threshold} = 1 \sim 15$. In (A) and (C), $g_x = 1 \sim 10$, $d_x = 1$ whereas in (B) and (D), we set $g_x = 5$ and $d_x = 0.1 \sim 3$.

From Fig 5(A), we observe that for a fixed event threshold, the mean FPT monotonically decreases with increasing the transcription rate (g_x), implying that the transcription

rate of protein X shortens the arriving time or accelerates the threshold crossing. On the other hand, for a fixed transcription rate (g_{x}), the mean FPT is a monotonically increasing function of event threshold, implying that the event threshold slows down the threshold crossing. By comparing Fig 5(B) with Fig 5(A), we can see that the change tendency in the case of degradation rate is fundamentally opposite to that in the case of transcription rate. From Fig 5(C), we observe that for a fixed event threshold, the variability in the timing is monotonically decreasing with the increase of transcription rate (g_{x}). We also observe from this panel that for a fixed transcription rate (g_{x}), the variability in the timing first decreases and then increases with the increase of event threshold. Fig 5(C) also shows a stair-like line, which is composed of the points corresponding to the least timing variability. From Fig 5(D), we also observe that for a fixed degradation rate (d_{x}), there exists a minimal timing variability. But for a fixed event threshold, the mean FPT is a monotonically increasing function of the degradation rate (d_{x}).

In a short, larger mean FPTs occur in the case of smaller transcription rates and larger event thresholds or in the case of larger degradation rates and larger event thresholds; the case for timing variability is almost converse to the case for mean FPT.

Optimal mean burst sizes for least timing variability

Here we investigate the influence of burst size on mean FPT and timing variability, with results shown in Fig 6. From Fig 6(A), we observe that the mean FPT is a monotonically decreasing function of mean burst size. Moreover, the curve corresponding to fluctuating threshold is always below the curve corresponding to fixed threshold, implying that dynamically fluctuating thresholds accelerate threshold crossing. Fig 6(B) shows the dependence of variability in timing on the mean burst size (b) for two different cases: fixed and fluctuating thresholds.

From this figure, we observe that there is optimal b such that the variability in the timing is least in both cases of threshold. This implies the mean burst size can make the timing precision reach optimality in both cases of fixed and fluctuating thresholds. In addition, we observe that there is a critical b (denoted by RP) such that the timing variability in the case of fluctuating threshold is smaller than that in the case of fixed

threshold, as b is beyond RP but the former is larger than the latter as the event threshold is below RP. In other words, for a small b, threshold fluctuations can reduce the timing variability or can raise the precision in the timing.

From Fig 6(C), we observe that larger mean FPTs appear in the region of the right-down corner, which corresponds to both smaller mean burst size and larger event thresholds. Specifically, for a fixed mean threshold, a larger mean burst size leads to the reduction of the mean FPT, implying that translation burst can accelerate response by shortening the arriving time. On the other hand, for a fixed mean burst size, a larger mean threshold leads to the increase of the mean FPT, implying that fluctuating threshold can slow down response by prolonging the arriving time. From Fig 6(D)(red curve), we observe that larger timing variability appears approximately in the region of the left-down corner, which corresponds to both smaller mean burst size and smaller event thresholds. Specifically, for a fixed small mean threshold, a smaller mean burst size leads to the increase of timing variability, implying that translation burst can slow down response by increasing the timing variability. However, there exists an optimal mean burst size such that the timing precision is best for almost large mean threshold. On the other hand, for a fixed large mean burst size(referring white curve in Fig 6(D)), a larger mean threshold leads to the decrease of the timing variability, implying that fluctuating threshold can enhance the timing precision by reducing the timing variability. However, there exists an optimal mean threshold such that the timing precision is best for almost large mean.

In short, translation burst (internal noise) accelerates threshold crossing, there is a critical mean burst size such that translation burst enhances the timing precision as the mean burst size is below this critical value but reduces the timing precision as the mean burst size is beyond this critical value, and there is an optimal mean burst size such that the timing precision is best.

Influence of absorbing domains on event timing

From the viewpoint of biology, a more reasonable absorbing domain is that apart from the condition of $x \geq y$, the condition of $x \geq x_C$ (a positive constant) is satisfied. This kind of absorbing domain can be mathematically described as $D_2 = \{(X, Y)|X(t) \geq Y(t), X(t) \geq$

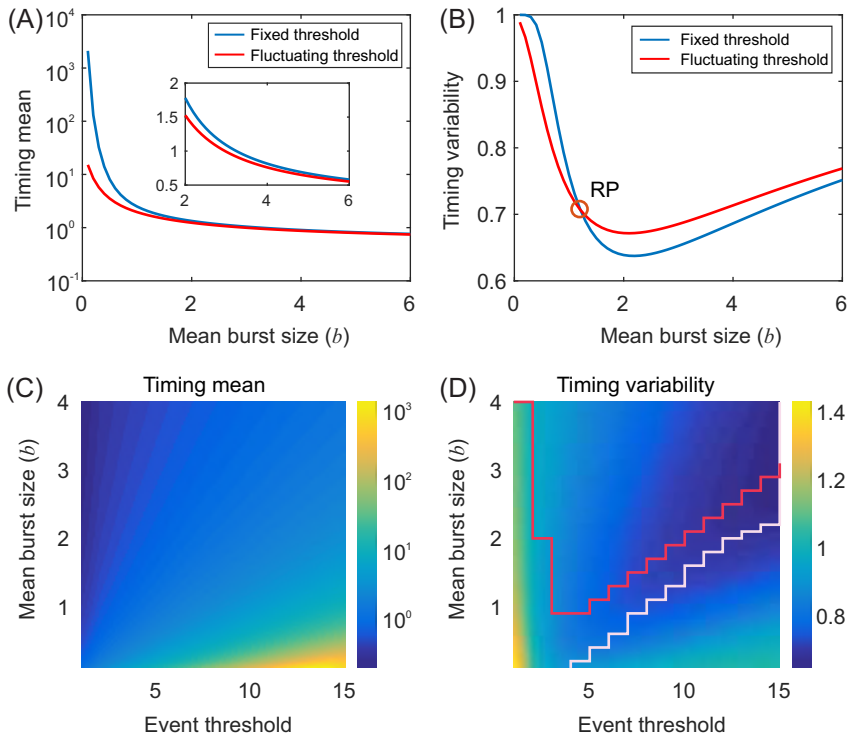

Fig 6. The effect of mean burst sizes on event timing. (A) Timing mean as a function of the mean burst size, where the inset shows a partial enlarged diagram. (B) Timing variability as a function of the mean burst size, where RP represents a critical point for reversing. (C) Heatmap showing timing mean as a function of event threshold and mean burst size. (D) Heatmap showing timing variability as a function of event threshold and mean burst size, where the red curve corresponds to the case that an event of threshold crossing has happened either due to a sufficiently large transcription rate (g_{x}) or due to a sufficiently small degradation rate (d_{x}), and the stair-like line consists of the points corresponding to the star in Fig 3(C) wherein a special value of g_{x} is used. In (A)-(D), the parameter values are set as $g_{\mathrm{x}} = 5$, $d_{\mathrm{x}} = 1$, $X_{\max} = 30$. In (A) and (B), the threshold is set as $Y_{\mathrm{threshold}} = g_{\mathrm{y}}/d_{\mathrm{y}}$ with $g_{\mathrm{y}} = 10$ and $d_{\mathrm{y}} = 1$, whereas in (C) and (D),$d_{\mathrm{y}} = 1$ and g_{y} is changed in $Y_{\mathrm{threshold}} = g_{\mathrm{y}}/d_{\mathrm{y}}$.

$x_C\}$ referring to the shadowed part in Fig 7(A) where the direction of crossing the threshold boundary is indicated, which depends on g_{x} and d_{y} according to the setting of our model. Similar to the analysis in the case of $D_1 = \{(X,Y)|X = X(t) \geq Y(t) = Y\}$, we can determine the absorbing domain of D_2 as well as the corresponding matrix $\mathbf{W}^{(1)}_{g_{\mathrm{x}}}$, $\mathbf{W}^{(2)}_{g_{\mathrm{x}}}$, $\mathbf{W}_{d_{\mathrm{y}}}$ (See the S1 Supporting Information for details). We point out that the latter kind of absorbing domain, which is different from the former kind of absorbing domain, can lead to complex threshold crossing events, raising a question: how does the timing of events depend on event threshold? Below, we simply address this question. Numerical results are demonstrated in Fig 7(B) and 7(C).

Fig 7(B) demonstrates the dependence of the mean FPT on event threshold. From

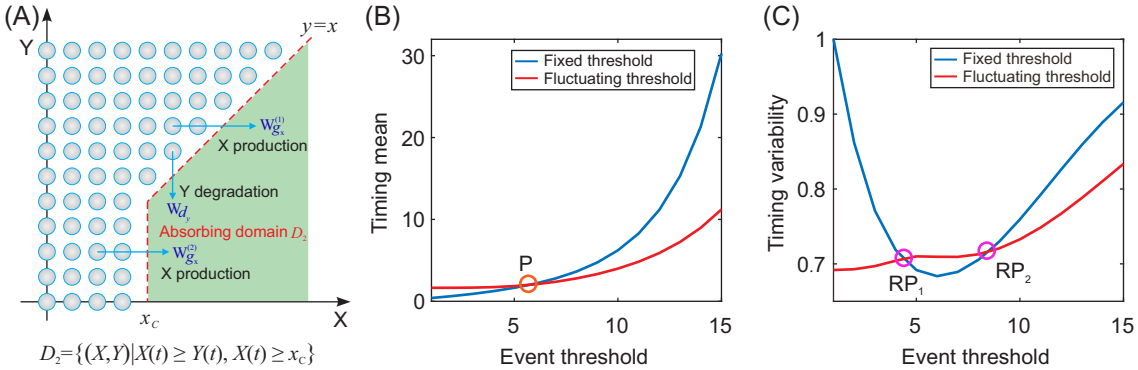

Fig 7. Comparison between the effects of fixed and fluctuating thresholds on timing in the case of the absorbing domain D_2. (A) Schematic for PFT when an absorbing domain is defined by $D_2 = \{(X, Y)|X(t) \geq Y(t),\ X(t) \geq x_C\}$ where arrows represent the direction of threshold crossing. (B) Timing mean as a function of event threshold for two different kinds of thresholds, where represents the crossing point P of two curves for the mean FPT in the two cases of event threshold. (C) Timing variability as a function of event threshold for two different kinds of thresholds, where two empty circle are the crossing point of two curves, denoted by RP_1 and RP_2. In (B) and (C), the parameter values are set as $x_C = 5$, $g_\mathrm{x} = 5$, $d_\mathrm{x} = 1$ and $b = 1$. The cutoff constant is set as $X_\mathrm{max} = 50$. If the fixed threshold is set as $Y_\mathrm{threshold} = 10$, the fluctuating threshold corresponds to $g_\mathrm{y} = 10$ and $d_\mathrm{y} = 1$.

this figure, we observe that the mean FPT is a monotonically increasing function of event threshold in both cases of threshold. Moreover, two dependence curves have the unique crossing point (P). If event threshold is larger than the threshold corresponding to point P, then the curve of the mean FPT vs. the event threshold in the case of fluctuations is below that of the mean FPT vs the event threshold in the case of no fluctuations, implying that threshold fluctuations can shorten the time that the regulatory proteins reach the critical threshold. If event threshold is smaller than the threshold corresponding to point P, then the curve of the mean FPT vs the event threshold in the case of fluctuations is beyond that of the mean FPT vs the event threshold in the case of no fluctuations, implying that threshold fluctuations can also prolong the time that the regulatory proteins reach the critical threshold. Fig 7(C) demonstrates how event threshold impacts variability in the timing. From this figure, we observe that the timing variability is in general larger in the case of no fluctuations than in the case of fluctuations, except for moderate event thresholds. Interestingly, there are two critical event thresholds, denoted by RP_1 and RP_2, such that the timing variability in the case of fluctuating threshold is smaller than that in the case of fixed threshold as the event threshold is below RP_1 or beyond RP_2. This implies that for a high

or low event threshold, fluctuations in threshold can reduce the timing variability or can raise the time precision. Comparing Fig 7(B)(case D_2) and 7(C) with Fig 3(A) and 3(C)(case D_1), we find that two new crossing points emerge in case D_2 (P in Fig 7(B) and RP_1 in 7(C)). The occurrence of these points stems from the fact that the absorbing domain D_2 shrinks under the constrained condition of both $X(t) \geq x_C$ and $X(t) \geq Y(t)$. Therefore, the results shown in Fig 7(B) and 7(C)) do not contradict to the qualitative result that threshold fluctuations accelerate threshold crossing and reduce timing variability. We also investigate the statistical properties of FPT in the other two cases of absorbing domains: $D_3 = \{(X,Y)|X(t) \geq Y(t), Y(t) \geq y_C\}$ and $D_4 = \{(X,Y)|X(t) \geq Y(t), X(t) \geq x_C, Y(t) \geq y_C\}\}$, with mathematical details and numerical results provided in the S1 Supporting Information.

Conclusion and Discussion

Many cellular processes including drug therapy involve event triggering or threshold crossing. Some of these processes require the precision in the timing that regulatory proteins reach thresholds, e.g., control of cell cycle, whereas the others depend on the time that regulatory proteins reach a threshold level (i.e., arrival time), e.g., apoptotic cells showed a faster accumulation of p53 than surviving cells and a shorter time to reach half-maximal p53 levels. Previous studies focused on precision in the timing of events in response to a fixed threshold [34–40]. However, the thresholds that biochemical events cross are in general dynamically fluctuating, as interpreted in the introduction. The noise in regulatory protein abundance and fluctuations in threshold can all lead to substantial cell-to-cell variability in timing. In this paper, we have systematically analyzed components essential for precision in timing of biochemical events at the level of single cells. Our approach relies on modeling event timing as the FPT for a stochastically expressed protein to cross a dynamically fluctuating threshold level. This framework was then used to reveal the mechanism of how the regulatory protein noise and threshold fluctuations altogether affect timing precision and arrival time. The main contributions and insights can be summarized as follows: (1) fluctuations in threshold accelerate response, and faster fluctuations lead to faster response; (2) there is an optimal mean threshold such that the variability is least; (3) there is an optimal mean burst size such

that the timing repression is best or the timing variability is smallest; (4) for a high enough threshold, the fluctuations in threshold can raise the timing precision; and (5) the timescales between transcription and degradation rates can adjust the precision in the timing, independent of the ratio of the transcription rate over the degradation rate. These results indicate that in contrast to fixed threshold, fluctuating threshold can significantly influence the timing of events.

How robust are the above results to noise sources and key modeling assumptions? For example, our model only considered the intrinsic noise in gene product levels but ignored the extrinsic noise in gene expression machinery [56, 57]. To incorporate such extrinsic noise, one may alter the transcription rate to $k_i Z$ (k_i is an external parameter), where Z may be drawn from an a priori probability distribution at the start of gene expression ($t = 0$) and remains fixed till the threshold is reached. Our model also ignored feedback regulation, which however exists widely in biological regulatory systems. Ghusinga, Dennehy and Singh [23] studied the influence of feedback regulation on the timing of events in the case of fixed threshold. They found that there is an optimal feedback strategy to regulate the synthesis of a protein to ensure that an event will occur at a precise time, while minimizing deviations or noise about the mean. In spite of this, how feedback regulation controls or impacts the timing of events in the case of dynamically fluctuating threshold is unclear. Using our analytical framework, one can also study the effect of feedback regulation on the timing of events in the case of dynamically fluctuating threshold. In our case, if changes in burst size, transcription rate or degradation rate are taken as the consequence of feedback regulation, the effect of feedback regulation on the timing of events will become clear in the case of fluctuating threshold.

Next, we simply discuss potential biological implications of our results in the context of fractional bacterial killing and p53 dynamics.

Connecting theoretical insights to fractional killing. Exposure of an isogenic bacterial population to a cidal antibiotic typically fails to eliminate a small fraction of refractory cells. In order to interpret this phenomenon, Roux J, et al. [26] investigated the basis of fractional cell killing by TRAIL and antibody agonists of DR4 and DR5 receptors. They demonstrated the existence of a threshold in initiator caspase activity (referred to as C8) that must be exceeded for cells to die. Interestingly, they found

that in cells that go on to die, C8 activity rises rapidly and monotonically until the threshold is reached and mitochondrial outer membrane permeabilization ensues, whereas in cells that survive, C8 activity rises more slowly for 1–4 h, never achieving the level required for death, and then falls back to pre-treatment levels over the next 4–8 h due to proteasome-mediated protein degradation. This finding, which can be reproduced by analysis of our model through the proposed approach, implies that Mycobacterium smegmatis can dynamically persist in the presence of a drug, and the stable number of cells characterizing this persistence was actually a dynamic state of balanced division and death.

Connecting theoretical insights to drug therapy. Many chemotherapeutic drugs kill only a fraction of cancer cells, limiting their efficacy. Paek AL, et al. [26] used live cell imaging to investigate the role of p53 dynamics in fractional killing of colon cancer cells in response to chemotherapy. They found that both surviving and dying cells reach similar levels of p53, indicating that cell death is not determined by a fixed p53 threshold. Instead, a cell's probability of death depends on the time and levels of p53. Cells must reach a threshold level of p53 to execute apoptosis, and this threshold increases with time. The increase in p53 apoptotic threshold is due to drug-dependent induction of anti-apoptotic genes, predominantly in the inhibitors of apoptosis family. While that study underlined the importance of measuring the dynamics of key players in response to chemotherapy to determine mechanisms of resistance and optimize the timing of combination therapy, our study here provided quantitative results for this importance.

Finally, our results illustrate the utility of the FPT framework for characterizing variability in the timing of key intracellular events and motivate alternative formulations of threshold crossing problems that might involve additional constraints such as fixing the time-integral of the underlying stochastic biochemical signal, rather than the original signal [58]. Exploring these constraints in more detail will be an important avenue for future research. In addition, analytical results and insights obtained here have broader implications for timing phenomenon in chemical kinetics, epidemic spreading, ecological modeling, and statistical physics.

Supporting information

S1 Supporting Information. Mathematical derivations and supplementary information. The derivation of all equations in the main text is provided, and more numerical results are demonstrated.

Acknowledgments

This work was supported by grants 91530320, 11775314, 11475273, and 11631005 from the National Natural Science Foundation of China; 2014CB964703 from the Science and Technology Department, P. R. China; 201707010117 from the Science and Technology Program of Guangzhou, P. R. China.

Author Contributions

Conceived and designed the experiments: JJ, TS. Performed the experiments: BH, JJ. Analyzed the data: BH, JJ, TS. Contributed reagents/materials/analysis tools: JJ, TS. Wrote the paper: JJ, TS.

References

1. Yurkovsky E, Nachman I. Event timing at the single-cell level. Briefings in Functional Genomics. 2013; 12: 90-98. https://doi.org/10.1093/bfgp/els057 PMID: 23196852

2. McAdams HH, Arkin A. Stochastic mechanisms in gene expression. Proceedings of the National Academy of Sciences. 1997; 94:814-819. https://doi.org/10.1073/pnas.94.3.814 PMID:9023339

3. Amir A, Kobiler O, Rokney A. Oppenheim AB, Stavans J. Noise in timing and precision of gene activities in a genetic cascade. Molecular Systems Biology. 2007; 3: 71. https://doi.org/10.1038/msb4100113 PMID: 17299413

4. Champlin DT, Truman JW. Ecdysteroid control of cell proliferation during optic lobe neurogenesis in the moth Manduca sexta. Development. 1998; 125:269-277. PMID:9486800

5. Dennehy JJ, Wang IN. Factors influencing lysis time stochasticity in bacteriophage lambda. BMC Microbiology. 2011; 11:174. https://doi.org/10.1186/1471-2180-11-174 PMID: 21810267

6. Koyama T, Iwami M, Sakurai S. Ecdysteroid control of cell cycle and cellular commitment in insect wing imaginal discs. Molecular and Cellular Endocrinology. 2004; 213:155-166. https://doi.org/10.1016/j.mce.2003.10.063 PMID:15062563

7. Carniol K, Eichenberger P, Losick R. A threshold mechanism governing activation of the developmental regulatory protein sigma σ^F in bacillus subtilis. Journal of Biological Chemical. 2004; 279:14860-14870. https://doi.org/10.1074/jbc.M314274200 PMID:14744853

8. Piggot PJ, Hilbert DW. Sporulation of bacillus subtilis. Current Opinion in Microbiology. 2004; 7:579-586. https://doi.org/10.1016/j.mib.2004.10.001 PMID:15556029

9. Spencer SL, Gaudet S, Albeck JG, Burke JM, Sorger PK. Non-genetic origins of cell-to-cell variability in TRAIL-induced apoptosis. Nature. 2009; 459:428-432. https://doi.org/10.1038/nature08012 PMID:19363473

10. Salz HK. Male or female? The answer depends on when you ask. PLoS Biology. 2007; 5:e335. https://doi.org/10.1371/journal.pbio.0050335 PMID:18162045

11. Goldschmidt Y, Yurkovsky E, Reif A, Rosner R, Akiva A, Nachman I. Control of relative timing and stoichiometry by a master regulator. PLoS ONE. 2015; 10(5):e0127339. https://doi.org/10.1371/journal.pone.0127339 PMID:26000862

12. Roux J, Hafner M, Bandara S, Sims JJ, Hudson H, Chai D, Sorger PK. Fractional killing arises from cell-to-cell variability in overcoming a caspase activity threshold. Molecular Systems Biology. 2015; 11: 803. https://doi.org/10.15252/msb.20145584 PMID:25953765

13. Cheng YY, Hirning AJ, Josić K, Bennett MR The timing of tanscriptional regulation in synthetic gene circuits. ACS Synthetic Biology. 2017, 6(11):1996–2002. https://doi.org/10.1021/acssynbio.7b00118 PMID:28841307

14. Aymoz D, Solé C, Pierre JJ, Schmitt M, de Nadal E, Posas F, Pelet S. Timing of gene expression in a cell-fate decision system. Molecular Systems Biology. 2018; 14(4):e8024. https://doi.org/10.15252/msb.20178024 PMID:29695607

15. Lin Y, Sohn CH, Dalal CK, Cai L, Elowitz MB. Combinatorial gene regulation by modulation of relative pulse timing. Nature. 2015; 527(7576):54-58. https://doi.org/10.1038/nature15710 PMID:26466562

16. Powell EO. An outline of the pattern of bacterial generation times. Journal of General Microbiology. 1958; 18:382-417. https://dx.doi.org/10.1099/00221287-18-2-382 PMID:13525657

17. Nachman I, Regev A, Ramanathan S. Dissecting timing variability in yeast meiosis. Cell. 2007; 131:544–556. https://doi.org/10.1016/j.cell.2007.09.044 PMID:17981121

18. Yosef N, Regev A. Impulse control: temporal dynamics in gene transcription. Cell. 2011; 144:886–896. https://doi.org/10.1016/j.cell.2011.02.015 PMID:21414481

19. Kuchina A, Espinar L, Çağatay T, Balbin AO, Zhang F, Alvarado A, Garcia-Ojalvo J, Süel GM. Temporal competition between differentiation programs determines cell fate choice. Molecular Systems Biology. 2011; 7:557. https://doi.org/10.1038/msb.2011.88 PMID:22146301

20. Bean JM, Siggia ED, Cross FR. Coherence and timing of cell cycle start examined at single-cell resolution. Molecular Cell. 2006; 21(1):3-14. https://doi.org/10.1016/j.molcel.2005.10.035 PMID:16387649

21. Chen KC, Calzone L, Csikasz-Nagy A, Cross FR, Novak B, Tyson JJ. Integrative analysis of cell cycle control in budding yeast. Molecular Biology of the Cell. 2004; 15:3841-3862. https://doi.org/10.1091/mbc.e03-11-0794 PMID:15169868

22. Liu X, Wang X, Yang X, et al. Reliable cell cycle commitment in budding yeast is ensured by signal integration. eLife. 2015; 4. https://doi.org/10.7554/eLife.03977.001 PMID:25590650

23. Schneider BL, Zhang J, Markwardt J, Tokiwa G, Volpe T, Honey S, et al. Growth rate and cell size modulate the synthesis of, and requirement for, G1-phase cyclins at start. Molecular and Cellular Biology. 2004; 24(24):10802-10813. https://doi.org/10.1128/MCB.24.24.10802-10813.2004 PMID:15572683

24. Di Talia S, Skotheim JM, Bean JM, Siggia ED, Cross FR. The effects of molecular noise and size control on variability in the budding yeast cell cycle. Nature. 2007; 448:947-951. https://doi.org/10.1038/nature06072 PMID:17713537

25. Wakamoto Y, Dhar N, Chait R, Schneider K, Signorino-Gelo F, Leibler S, McKinney JD. Dynamic persistence of antibiotic-stressed mycobacteria. Science. 2013; 339:91-95. https://doi.org/10.1126/science.1229858 PMID:23288538

26. Paek AL, Liu JC, Loewer A, Forrester WC, Lahav G. Cell-to-cell variation in p53 dynamics leads to fractional killing. Cell. 2016; 165:631-642. https://doi.org/10.1016/j.cell.2016.03.025 PMID:27062928

27. Raser JM, O'Shea EK. Noise in gene expression: origins, consequences, and control. Science. 2005; 309:2010-2013. https://doi.org/10.1126/science.1105891 PMID:16179466

28. Raj A, van Oudenaarden A. Nature, nurture, or chance: stochastic gene expression and its consequences. Cell. 2008; 135:216-226. https://doi.org/10.1016/j.cell.2008.09.050 PMID:18957198

29. Eldar A, Elowitz MB. Functional roles for noise in genetic circuits. Nature. 2010; 467:167-173. https://doi.org/10.1038/nature09326 PMID:20829787

30. Snijder B, Pelkmans L. Origins of regulated cell-to-cell variability. Nature Reviews Molecular Cell Biology. 2011; 12:119-125. https://doi.org/10.1038/nrm3044 PMID:21224886

31. Zhang JJ, Zhou TS. Promoter-mediated transcriptional dynamics. Biophysical Journal. 2014; 106:479-488. https://doi.org/10.1016/j.bpj.2013.12.011 PMID:24461023

32. Liu TQ, Zhang JJ, Zhou TS. Effect of interaction between chromatin loops on cell-to-cell variability in gene expression. PLoS Computational Biology. 2016; 12(5):e1004917. https://doi.org/10.1371/journal.pcbi.1004917 PMID:27153118

33. Griffth JS. Mathematics of cellular control processes I. Negative feedback to one gene. Journal of Theoretical Biology. 1968; 20:209–216. https://doi.org/10.1016/0022-5193(68)90189-6 PMID:5727239

34. Ghusinga KR, Dennehy JJ, Singh A. First-passage time approach to controlling noise in the timing of intracellular events. Proceedings of the National Academy of Sciences. 2017; 114(4):693-698. https://doi.org/10.1073/pnas.1609012114 PMID: 28069947

35. Co AD, Lagomarsino MC, Caselle M, Osella M. Stochastic timing in gene expression for simple regulatory strategies. Nucleic Acids Research. 2017; 45(3):1069-1078. https://doi.org/10.1093/nar/gkw1235 PMID:28180313

36. Gupta S, Varennes J, Korswagen HC, Mugler A. Temporal precision of regulated gene expression. PLoS Computational Biology. 2018; 14(6):e1006201. https://doi.org/10.1371/journal.pcbi.1006201 PMID:29879102

37. Singh A, Dennehy JJ. Stochastic holin expression can account for lysis time variation in the bacteriophage λ. Journal of The Royal Society Interface. 2014; 11(95):20140140. https://doi.org/10.1098/rsif.2014.0140 PMID:24718449

38. Murugan R, Kreiman G. On the minimization of fluctuations in the response times of autoregulatory gene networks. Biophysical Journal. 2011; 101:1297-1306. https://doi.org/10.1016/j.bpj.2011.08.005 PMID:21943410

39. Bel G, Munsky B, Nemenman I. The simplicity of completion time distributions for common complex biochemical processes. Physical Biology. 2009; 7(1):016003. https://doi.org/10.1088/1478-3975/7/1/016003 PMID:20026876

40. Iyer-Biswas S, Zilman A. First-passage processes in Cellular Biology. Advances in Chemical Physics. 2016; 160(Chap.5):261-306 https://doi.org/10.1002/9781119165156.ch5

41. Taillefumier T, Magnasco MO. A phase transition in the first passage of a Brownian process through a fluctuating boundary with implications for neural coding. Proceedings of the National Academy of Sciences. 2013; 110(16):E1438-1443. https://doi.org/10.1073/pnas.1212479110 PMID:23536302

42. Tuckwell HC, Wan FYM. First-passage time of Markov processes to moving barriers. Journal of Applied Probability. 1984; 21:695-709. https://doi.org/10.2307/3213688

43. Doering CR, Gadoua JC. Resonant activation over a fluctuating barrier. Physical Review Letters. 1992; 69(16):2318-2321. https://doi.org/10.1103/PhysRevLett.69.2318 PMID:10046454

44. Lo CF, Hui CH. Computing the first passage time density of a time-dependent Ornstein-Uhlenbeck process to a moving boundary. Applied Mathematics Letters. 2006; 19(12):1399–1405. https://doi.org/10.1016/j.aml.2006.02.011

45. Redner S. A Guide to First-passage processes. Cambridge: Cambridge University Press; 2001. https://doi.org/10.1017/CBO9780511606014

46. Metzler R, Oshanin G, Redner S, eds. First-passage phenomena and their applications. Singapore: World Scientific; 2014. https://doi.org/10.1142/9104

47. Gardiner C. Stochastic methods: a handbook for the natural and social sciences. 4th ed. New York: Springer; 2009.

48. Van Kampen N. Stochastic process in physics and chemistry. 3rd ed. North-Holland, Amsterdam; 2007.

49. Berg OG. A model for the statistical fluctuations of protein numbers in a microbial population. Journal of Theoretical Biology. 78; 71:587-603. https://doi.org/10.1016/0022-5193(78)90326-0 PMID:96307

50. Yu J, Xiao J, Ren X, Lao K, Xie XS. Probing gene expression in live cells, one protein molecule at a time. Science. 2006; 311(5767):1600-1603. https://doi.org/10.1126/science.1119623 PMID:16543458

51. Cai L, Friedman N, Xie XS. Stochastic protein expression in individual cells at the single molecule level. Nature. 2006; 440(7082):358-362. https://doi.org/10.1038/nature04599 PMID:16541077

52. Shahrezaei V, Swain PS. Analytical distributions for stochastic gene expression. Proceedings of the National Academy of Sciences. 2008; 105:17256–17261. https://doi.org/10.1073/pnas.0803850105 PMID:18988743

53. Munsky B, Khammash M. The finite state projection algorithm for the solution of the chemical master equation. The journal of chemical physics. 2006; 124(4):044104. https://doi.org/10.1063/1.2145882 PMID:16460146

54. Gillespie DT. Exact stochastic simulation of coupled chemical-reactions. The Journal of Physical Chemistry. 1977; 81:2340-2361. https://doi.org/10.1021/j100540a008

55. Gammaitoni L, Hänggi P, Jung P, Marchesoni F. Stochastic resonance. Reviews of Modern Physics. 1998; 70(1):223-287. https://doi.org/10.1103/RevModPhys.70.223

56. Shahrezaei V, Ollivier JF, Swain PS. Colored extrinsic fluctuations and stochastic gene expression. Molecular Systems Biology. 2008;4:196. https://doi.org/10.1038/msb.2008.31 PMID:18463620

57. Singh A. Transient changes in intercellular protein variability identify sources of noise in gene expression. Biophysical Journal. 2014; 107:2214-2220. https://doi.org/10.1016/j.bpj.2014.09.017 PMID:25418106

58. Jafarpour F, Vennettilli M, Iyer-Biswas S. Biological timekeeping in the presence of stochasticity. arXiv preprint. 2017; arXiv:1703.10058v1.